AD-A129 489 STOICHIOMETRY AND CONDUCTIVITY RESPONSE OF AMORPHOUS AND CRYSTALLINE COMP..(U) NORTHWESTERN UNIV EVANSTON IL MATERIALS RESEARCH CENTER M STAINER ET AL. 09 MAY 83 1/1

UNCLASSIFIED F/G 11/9 NL

END
DATE
FILMED
DTIC

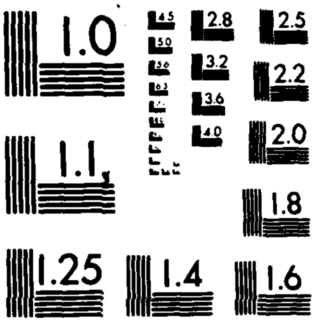
1.0
4.5
5.0
5.6
6.3
2.8
3.2
3.6
4.0
2.5
2.2
2.0
1.1
1.8
1.25
1.4
1.6

SECURITY CLASSIFICATION OF THIS PAGE (When Data Entered)

REPORT DOCUMENTATION PAGE

READ INSTRUCTIONS BEFORE COMPLETING FORM

1. REPORT NUMBER: 007
2. GOVT ACCESSION NO: AD-A129489
3. RECIPIENT'S CATALOG NUMBER:
4. TITLE (and Subtitle): Stoichiometry and Conductivity Response of Amorphous and Crystalline Complexes formed Between Poly(ethylene oxide) and Ammonium Salts
5. TYPE OF REPORT & PERIOD COVERED: Interim Technical Report
6. PERFORMING ORG. REPORT NUMBER:
7. AUTHOR(s): M. Stainer, L. C. Hardy, D. H. Whitmore, and D. F. Shriver
8. CONTRACT OR GRANT NUMBER(s): N00014-80-C-0532
9. PERFORMING ORGANIZATION NAME AND ADDRESS: Department of Chemistry and Materials Research Center, Northwestern University, Evanston, Illinois 60201
10. PROGRAM ELEMENT, PROJECT, TASK AREA & WORK UNIT NUMBERS: NR 359-746
11. CONTROLLING OFFICE NAME AND ADDRESS: Office of Naval Research, Department of Navy, Arlington, Virginia 22217
12. REPORT DATE: 9 May 1983
13. NUMBER OF PAGES:
14. MONITORING AGENCY NAME & ADDRESS (if different from Controlling Office):
15. SECURITY CLASS. (of this report):
15a. DECLASSIFICATION/DOWNGRADING SCHEDULE
16. DISTRIBUTION STATEMENT (of this Report): Approved for public release and sale. Distribution unlimited.
17. DISTRIBUTION STATEMENT (of the abstract entered in Block 20, if different from Report):
18. SUPPLEMENTARY NOTES: Submitted to the Journal of the Electrochem. Soc.

DTIC
ELECTE
JUN 17 1983
S D
E

19. KEY WORDS (Continue on reverse side if necessary and identify by block number): Solid electrolytes, polymer electrolytes Poly(ethylene oxide), polymer salt complexes
20. ABSTRACT (Continue on reverse side if necessary and identify by block number)

A single crystalline phase having the approximate composition 4:1 PEO$\cdot NH_4SCN$ was identified, and an approximate phase diagram was constructed. The PEO$\cdot NH_4SO_3CF_3$ system is more complex and a phase diagram was not obtained however at least two compounds of 8:1 and 4:1 stoichiometry are indicated. Conductivity plots indicate that the metastable amorphous phase of the various materials has a conductivity approximately 10^3 higher than that of the crystalline phase at room temperature.

DD FORM 1 JAN 73 1473 EDITION OF 1 NOV 65 IS OBSOLETE
S/N 0102-LF-014-6601

SECURITY CLASSIFICATION OF THIS PAGE (When Data Entered)

20 Continued. (Abstract Continued.)

implicated as a charge carrier.

Stoichiometry and Conductivity Response of Amorphous and Crystalline Complexes Formed Between Poly(ethylene oxide) and Ammonium Salts: PEOx·NH_4SCN and PEOx·$NH_4SO_3CF_3$

Matthew Stainer, L. Charles Hardy, D. H. Whitmore, and D. F. Shriver
Departments of Chemistry and Material Science and Materials Research Center
Northwestern University, Evanston, Illinois 60201

Abstract

Stoichiometries have been studied for the interaction between poly(ethylene oxide), and the ammonium salts NH_4SCN and $NH_4SO_3CF_3$, in the polymer to salt composition range 10:1 to 2:1. A single crystalline phase having the approximate composition 4:1 PEO·NH_4SCN was identified, and an approximate phase diagram was constructed. The PEO·$NH_4SO_3CF_3$ system is more complex and a phase diagram was not obtained however at least two compounds of 8:1 and 4:1 stoichiometry are indicated. Conductivity plots indicate that the metastable amorphous phase of the various materials has a conductivity approximately 10^3 higher than that of the crystalline phase at room temperature. The NH_4^+ ion rather than H^+ is implicated as a charge carrier. We were not successful in determining transferrence numbers for anions and cations.

Introduction

Recently solvent free polymer electrolytes have attracted considerable attention becuase of their potential application in high energy density batteries and because of the many unanswered fundamental questions on ion transport in polymers [1-4]. The temperature dependent conductivity of amorphous polyether-salt complexes reveals curved plots of $\ln(\sigma T)$ vs $1/T$, which are linear when the temperature variable $1/(T-T_o)$ is employed. This functional dependence of the ion transport has previously been observed for small molecule diffusion through polymers, and one possible interpretation is that cooperative polymer conformation fluctuations are responsible for the transport process. The empirical constant T_o represents the temperature below which the polymer motions responsible for ion transport are frozen out and therefore it is approximately equal to the glass transition temperature, T_g. The $1/(T-T_o)$ dependence is reproduced by the configurational entropy model of Gibbs and co-workers, which gives equation (1) for the conductivity.

$$\sigma = AT^{-1/2}\exp\{-K/T-T_o\} \quad (1)$$

$$\text{where } K = T_o \Delta\mu S_c{}^*/k_B B \quad (2)$$

A, T_O, and B are constant, $S_c{}^*$ is the minimum configurational entropy required for rearrangement, and k_B is the Boltzman constant. The pre-exponential term, A, is proportional to the carrier concentration [5].

Most of the research to date has focused on lithium and sodium ion conductors where the respective metals may be used as reversible electrodes [6-8]. In the present work, ammonium ion has been chosen for study because little is known about the transport of proton-containing species in polymer electrolytes.

Also, the ammonium-containing poly(ethylene oxide), (PEO), systems provide metastable amorphous phases which are useful for testing theories on ion transport. This research has focused on the stoichiometry of interaction between NH_4SCN or $NH_4SO_3CF_3$ and PEO, and a comparison of ion transport in the crystalline and amorphous states of these polymer electrolytes.

The size of the NH_4^+ ion is interesting in its relationship to structural models for PEO-salt complexes which have been presented to date. The most convincing model indicates that cations Li^+, Na^+, or K^+ reside in a helical tunnel and are coordinated to oxygen atoms in a fashion very similar to cations in an 18-crown-6 complex [9], where the cavity size for each is essentially the same (diameter ~ 2.6 Å for PEO complex and for 18-crown-6). Until recently, X-ray crystal structures of many 18-crown-6 complexes of ammonium and rubidium salts have indicated that these cations, both with a radius of 1.48 Å, are too large to fit in the cavity, but sit on top of it. Recent structures of 18-crown-6 with ammonium ions indicate that this assertion is incorrect and instead the depth of penetration of the crown ether by an ammonium ion depends on the relative strength of interaction of the ion surrounding groups [10]. Hydrogen bonding is an important interaction here.

Complexes of PEO with rubidium and cesium salts have been reported to be amorphous, unlike the crystalline complexes obtained when using the smaller alkali metal cations Na^+ and K^+ [9]. An explanation for this behavior might be that since the cations do not fit inside the helical cavity, the structure is not regular and therefore not crystalline. Also, irregular crosslinking of the polyether backbone through interactions with cations may induce the amorphous structure. But RbI has been shown to form a crystalline complex with an eight-oxygen polyether capped by aromatic end groups; the polyether is wrapped around the cation in a helical fashion. This complex is originally obtained as an oil which slowly recrystallizes. Under similar conditions with NH_4SCN substituted for RbI as the complexing salt, crystals were not obtained [11].

The evidence indicates that size and hydrogen-bonding ability play important roles in interactions of NH_4^+ with short chain polyethers and possibly with PEO. From the previous information, it would be difficult to predict the exact stoichiometry of interaction of ammonium salts with PEO. Anion differences, which would affect crystal packing, might also be expected to play an important role. For example, the complex $PEO \cdot Na[B(C_6H_5)_4]$ has a maximum ratio of ether oxygens to Na^+ of about 7:1 due to the bulky anion [12].

Experimental

Materials. Poly(ethylene oxide) (PEO), average molecular weight 600,000 (Aldrich) was purified and dried as described previously [9]. Reagent grade NH_4SCN was dried under vacuum at 100°C for 19 hr. $NH_4SO_3CF_3$ was prepared by neutralization of freshly distilled HSO_3CF_3 to pH 6 with ammonium hydroxide, recrystallization from THF/hexane, and drying under vacuum for 24 hr. $ND_4SO_3CF_3$ was prepared from $NH_4SO_3CF_3$ and D_2O. Due to the hygroscopic nature of these salts and purified PEO, all operations were carried out in a nitrogen atmosphere dry box or using standard Schlenk techniques. Anhydrous salts were checked for signs of water by IR prior to use. Reagent grade methanol (MCB) was dried by refluxing over iodine-activated magnesium for one day followed by distillation under a nitrogen atmosphere. Tungsten bronze, $(NH_4)_xWO_3$ ($x \approx 0.25$), was prepared by reduction of ammonium paratungstate in hydrogen atmosphere (300 Torr) at $\sim$500°C by the method of Dickens, et al [13].

The polymer electrolytes were prepared typically on a 0.5 g scale by combining stoichiometric quantities of the polymer and salt and addition of 15 mL anhydrous methanol. The mixture was stirred until all solids dissolved. Dissolution indicates complexation since PEO is not soluble in methanol. The solvent was removed by evaporation under vacuum and dried under high vacuum (10^{-3} torr) for 24 hr.

Differential Scanning Calorimetry (DSC). Thermal analysis of PEO-ammonium salt electrolytes was carried out using a Perkin Elmer DSC-2 differential scanning calorimeter on a range of 1 (mcal/sec) with a heating rate of 10 K/min unless otherwise noted. Endothermic transition temperatures were determined by the intersection of a line drawn through the leading edge of the fusion peak with an extrapolated base line. Samples were typically 1-4 mg and loaded under a nitrogen atmosphere in hermetically sealed aluminum pans. Peak shape and location depend somewhat on packing, geometry, and size of sample which could not be well controlled since samples were either films or cut from chunks.

An iridium standard was used to calibrate the DSC-2 temperature scale and for heat of fusion calculations. After each scan, samples were quenched at 320 K/min down to 300 K. The samples were then rescanned using the original conditions. After recrystallization from the melt (time dependent on stoichiometry and salt) samples were scanned again.

Optical Polarized Microscopy. Crystalline-amorphous state changes were observed using optical polarized microscopy. A Leitz Wetzlar polarizing microscope equipped with a Mettler FP52 hot stage was used to observe the disappearance of birefringence. Samples were prepared by hot pressing electrolyte material between a microscope slide and cover slip and sealing with epoxy in a nitrogen atmosphere.

X-ray Diffraction Measurements. X-ray diffraction measurements were obtained with a Rigaku automated diffractometer and radiation analyzer using CuKα radiation. Symmetrical reflection was used on pressed pellets which were held in place and protected from atmospheric moisture by Scotch-brand transparent tape. A beryllium window was used for the sample side exposed to X-rays.

Conductivity Measurements. A.C. impedance measurements over the frequency range 50 Hz-500 kHz were made using a Hewlett Packard 4800A vector impedance meter. Polymer samples were pressed at 10,000 psi in a 1/2" diameter die (thickness 1-2 mm) and loaded in a sealed sample holder between either 0.2 mm thick Pt discs or $(NH_4)_{0.25}WO_3$ electrodes which were 1/2" diameter pellets ($\sim$2 mm thick) pressed from finely ground powder. Variable temperature measurements between 25°C and 100°C were carried out with the sample in a thermostatted heating chamber controlled by a Bruker B-ST temperature control unit.

Results and Discussion

Polymer-Salt Phases. The X-ray diffraction patterns of various stoichiometries of $PEO \cdot NH_4SCN$ mixtures are shown in Figure 1. Comparison of the pattern of the 8:1 composition with that of pure PEO indicates the presence of uncomplexed crystalline PEO in addition to crystalline polymer salt complex. At high salt concentrations, 3:1 and 2:1 compositions, reflections arising from the presence of free salt are seen. The pattern for $PEO_{4.0}NH_4SCN$ does not contain reflections of either free salt or uncomplexed polymer.

Differential scanning calorimetry experiments confirm the conclusion, drawn from the X-ray results, that a crystalline complex is formed between salt and polymer with the approximate stoichiometry of $PEO_{4.0}NH_4SCN$. The DSC thermograms are shown in Figure 2. A single sharp endotherm at 68°C is found for $PEO_{4.0}NH_4SCN$. Optical microscopy experiments show that this endotherm corresponds to the melting of the crystalline complex. Decreasing the salt concentration successively to the 5:1 and 6:1 compositions gives a relative decrease in the magnitude of the 68°C endotherm and the appearance of an endotherm at ~42°C. The latter can be assigned to the eutectic melting of a mixture of $PEO_{4.0}NH_4SCN$ and PEO. Optical microscopy also shows that this represents the transition from a crystalline to an amorphous phase. The phase diagram for the PEO-NH_4SCN system is shown in Figure 3. The melting points of NH_4SCN and PEO 600,000 are 149°C and 65°C, respectively. The complex $PEO_{4.0}NH_4SCN$ melts at 68°C and the temperature of the eutectic melt is 42°C. The endotherm at ~95°C in the DSC thermogram of the 3:1 composition does not arise from the polymer-salt interaction but is assigned on the basis of optical microscopy to a phase transition in crystalline NH_4SCN [14].

In contrast to the data for 8:1 PEO·NH_4SCN, the X-ray diffraction pattern of 8:1 PEO·$NH_4SO_3CF_3$ does not contain reflections assignable to free PEO. The DSC thermogram for this complex, Figure 5, shows a single endotherm at 41°C. The failure to detect uncomplexed PEO by X-ray powder diffraction suggests that the thermal event observed at 41°C is not a eutectic melting as was found for the NH_4SCN case but corresponds to the crystalline-amorphous phase transition of a polymer-salt complex. Increasing the salt concentration to the 4:1 composition gives a second higher temperature endotherm in the DSC traces at 60°C, Figure 5. This is assigned to the crystalline melt of a second polymer salt complex phase corresponding roughly to 4:1 polymer to salt stoichiometry similar to that found in the PEO-NH_4SCN system. Although a single endotherm is seen in the DSC at a composition of 10:1, evidence for the presence of small amounts of PEO is seen in optical microscopy and X-ray diffraction. The diffraction pattern, Figure 4, is essentially identical to that of 8:1 PEO·$NH_4SO_3CF_3$ with the exception of an additional reflection which corresponds to one of the two strong reflections found for PEO. Comparison of the X-ray diffraction patterns of the 8:1 and the 5:1 stoichiometries reveals a close similarity with additional strong reflections being found for the latter. This is consistent with the DSC results which indicate that both of the crystalline complex phases are present at the 5:1 stoichiometry. Similarly the diffraction pattern of the 3:1 stoichiometry is much different from that of the 8:1 supporting the DSC result which shows that the low salt concentration complex phase is absent at the 3:1 stoichiometry. Interestingly, the 3:1 and 2:1 compositions do not appear, from the X-ray data, to contain free uncomplexed salt. This behavior contrasts with the NH_4SCN system and thus the endotherm at 94°C seen in the DSC traces at high concentrations of $NH_4SO_3CF_4$ may possibly arise from a further polymer·salt complex phase.

The rates of recrystallization of the polymer·salt phases are slow. Rescanning of the DSC samples, after quenching and equilibration at room temperature, gives thermograms in which the 41°C and 60°C endotherms are absent. The rates of crystallization vary with polymer:salt stoichiometry and anion. For the $NH_4SO_3CF_3$ complexes crystallization from the melt is complete after 24 hours, the low salt stoichiometry phase crystallizing more slowly. In the case of NH_4SCN the rates are slower on the order of weeks for the 8:1 and 6:1 stoichiometries and a few days for 4:1. For $PEO_{3.0}NH_4SO_3CF_3$ the endotherm at ~94°C is seen on immediate rescanning while the endotherm at 57°C is absent.

Conductivity Measurements.

Measurements of the conductivity of the PEO ammonium ion complexes were carried out at temperatures between 25 and 100°C. Plots of $\ln(\sigma T)$ vs $1/T$ for NH_4SCN and $NH_4SO_3CF_3$ complexes of various stoichiometries are shown in Figures 6 and 7, respectively. Perhaps the most striking features are the steep rises in conductivity over relatively small temperature intervals which occur when the crystalline complexes are heated. For $PEO_{8.0}NH_4SCN$ this sharp rise occurs at about 45°C. Similarly for the 5:1 complex there is a pronounced rise at ~45°C with a smaller inflection at ~72°C while for the 4:1 only a single sharp rise in conductivity is observed at ~72°C. This latter transition has been observed previously for the 4:1 complex [15], but no conductivity was reported for the amorphous state. For the 3:1 stoichiometry, the inflection is slightly elevated to ~80°C due to the presence of excess salt. This behavior parallels the endothermic events seen in the DSC measurements which correspond to the crystalline to amorphous phase transitions. Conductivity plots of the $PEO\cdot NH_4SO_3CF_3$ complexes, Figure 7, show the same features with sharp rises or inflections corresponding to features in the DSC traces, Figure 5. The slow recrystallization of the complexes from the amorphous melt facilitates the measurement of the conductivity in that phase below the crystalline melting temperature. Cooling to room temperature and remeasuring the conductivities between 25°C and 100°C gives the curves, Figures 6b and 7b. Notable is the large enhancement is conductivity in the amorphous phase over that in the crystalline material, about a factor of 10^3 at room temperature. Also for the amorphous phase the curve is not strictly linear but is slightly bowed and thus the system does not exhibit true Arrhenius behavior. The transitions seen in the conductivity plots are reproducible after recrystallization.

Conductivity in PEO-salt complexes has been shown to be essentially ionic in nature [6]. The relative mobilities of cation and anion however are of particular importance especially in relation to the practical applications of polymer electrolytes in energy storage devices. Weston and Steele have shown that in 8:1 $PEO \cdot LiClO_4$ complexes the transport number for the lithium ions is less than 0.5 [7] and Sorensen and Jacobsen have found a cation transport number of 0.54 in $PEO_{4.5}LiSCN$ [8].

As indicated below, ionic motion in $PEO \cdot NH_4X$ probably does not involve proton transfer from NH_4^+ to the polyether polymer backbone. The conductivity behavior of $PEO_{4.0}ND_4SO_3CF_3$ is essentially identical to that for the normal isotopic ammonium complex and there is no increase in the slope of the Arrhenius plots due to an isotope effect. Therefore a transport mechanism involving proton transfer seems unlikely.

An experiment was performed in which a polymer complex was doped with ammonia because the presence of free NH_3 might provide a mechanism for proton transport. The polymer salt complex absorbs ammonia readily and swells and exhibits mechanical properties similar to those of an undoped polymer salt complex in the amorphous phase. No enhancement of conductivity was observed. The ammonia doped polymer has roughly the same conductivity as the undoped material in the amorphous phase again indicating that H^+ conductivity is not occurring. Finally evidence for the mobility of NH_4^+ was obtained using ion reversible and ion blocking electrodes. Figure 8 shows the AC complex admittance plots for 5:1 PEO$\cdot NH_4SO_3CF_3$ in the frequency range 50 x 10^4 Hz to 50 Hz with Pt (blocking) and $(NH_4)_{0.25}WO_3$ (reversible) electrodes. The latter electrode material is reversible to NH_4^+ ions and shows the "spur" typical of an arrangement where the double layer capacitance at the electrode-electrolyte interface is removed by reversible transfer of NH_4^+ ions. The ammonium ions are thus clearly implicated as a mobile species in these polymer electrolytes. However we were unsuccessful in determining the transport number with a polarization cell having ammonium tungsten bronze electrodes, so it is possible that the anion contributes substantially to the conductivity.

Conclusion

Although determining the stoichiometry of interaction has been an important segment of this work, the most significant aspect has been determining the conductivity behavior of these materials in their crystalline and metastable, amorphous states. In the amorphous state, conductivity enhancement at room temperature is roughly $10^3\ \Omega^{-1}cm^{-1}$ greater than for the corresponding crystalline state of these electrolytes. This behavior strengthens the assumption that cooperative polymer conformation fluctuations are responsible, at least in part, for the transport process in these conductors. Such a large conductivity enhancement indicates that other amorphous solid electrolytes above their T_g's might be very promising as fast ionic conductors.

Other comparisons of crystalline vs. amorphous conductivity in the same electrolyte have been reported [7,15]. But in the PEO$\cdot LiClO_4$ 8:1 comparison

[7], the amorphous state was induced by the addition of water so the true comparison of conductivities may be difficult to make since water is known to increase conductivity. In another report [15] slightly higher conductivities due to annealing above the melting point of the electrolyte PEO·$LiClO_4$ 8:1 or PEO·$LiSO_3CF_3$ 8.1:1 are suggested to be due to slow recrystallization, but this conclusion is not confirmed by other means.

Acknowledgment

This research was supported by the NSF Materials Research Laboratory Program through the Northwestern University Materials Research Center and by the Office of Naval Research. We appreciate helpful conversations with Professors Mark Ratner and Buckley Crist.

References

1. R. W. Dupon, B. L. Papke, M. A. Ratner, D. H. Whitmore, and D. F. Shriver, *J. Am. Chem. Soc.*, **104**, 6247 (1982).
2. C. C. Lee and P. V. Wright, *Polymer*, **23**, 681 (1982).
3. M. B. Armand, Proceedings of the Workshop on Lithium Nonaqueous Battery Electrochemistry. Cleveland, Ohio; June 1980, pp. 261.
4. J. E. Weston and B. C. H. Steele, *Solid State Ionics*, **7**, 75 (1982).
5. B. L. Papke, M. A. Ratner, and D. F. Shriver, this Journal, **129**, 1694 (1982).
6. R. W. Dupon, D. H. Whitmore, and D. F. Shriver, this Journal, **128**, 715 (1981).
7. J. E. Weston and B. C. H. Steele, *Solid State Ionics*, **7**, 81 (1982).
8. P. R. Sorensen and T. Jacobsen, *Electrochimica Acta*, **27**, 1671 (1982).
9. B. L. Papke, M. A. Ratner, and D. F. Shriver, *J. Phys. Chem. Solids*, **42**, 493 (1981).
10. K. N. Trueblood, C. B. Knobler, D. S. Lawrence, and R. V. Stevens, *J. Am. Chem. Soc.*, **104**, 1355 (1982) and references therein.
11. G. Weber, W. Saenger, F. Vögtle, and H. Sieger, *Angew. Chem. Int. Ed. Engl.*, **18**, 227 (1979).
12. B. L. Papke, Ph.D. Thesis, Northwestern University, 1982.
13. P. G. Dickens, A. C. Halliwell, D. J. Murphy, and M. S. Whittingham, *Trans. Faraday Soc.* **67**, 794 (1971).
14. Y. Kinsho, Onodera, M. Sakiyama, and S. Seki *Bull. Chem. Soc. Jpn.*, **52**, 395 (1979)
15. P. V. Wright, *Br. Polym. J.*, **7**, 319 (1975).
16. J. E. Weston and B. C. H. Steele, *Solid State Ionics*, **2**, 347 (1981).

Figure Captions

Fig. 1. X-ray diffraction patterns for NH_4SCN (upper trace), poly(ethylene oxide) (lower trace), and complexes between poly(ethylene oxide) and NH_4SCN (center traces). The ratios of PEO to NH_4SCN are indicated.

Fig. 2. Differential scanning calorimetric scans of the poly(ethylene oxide)-ammonium thiocyanate system. The ratio of polymer to salt is indicated. The heating rate was 10°C/min. in each scan.

Fig. 3. Approximate phase diagram for the $PEO \cdot NH_4SCN$ system. The 4:1 ($PEO \cdot NH_4SCN$) complex, shown at 0.2 mole fraction of salt, may exist over a range of stoichiometry but this was not readily established.

Fig. 4. X-ray diffraction patterns for $NH_4SO_3CF_3$ (upper trace), PEO (lower trace) and complexes formed between these constituents (center traces). The ratios of PEO to $NH_4SO_3CF_3$ are indicated.

Fig. 5. Differential scanning calorimetric thermograms of the $PEO-NH_4SO_3CF_3$ system. The ratio of polymer to salt are indicated. The heating rate was 10°C min^{-1} in each scan.

Fig. 6. Electrical conductivity, σ, versus temperature plotted as $\ln(\sigma T)$ vs. $1000/T$, for crystalline and amorphous phases of $PEO \cdot NH_4SCN$ at various ratios of polymer to salt: Δ, 8:1; O, 5:1; X, 4:1; □, 3:1. a) Crystalline material. Measurements made starting at room temperature and heating to 100°C. Dashed line indicates conductivities in the amorphous phase shown in b. b) Amorphous material. After quenching the sample from 100°C to room temperature, conductivities were measured starting at room temperature and heating to 100°C.

Fig. 7. Electrical conductivity, σ versus temperature plotted as $\ln(\sigma T)$ vs. 1000/T, for crystalline and amorphous phases of $PEO \cdot NH_4SO_3CF_3$ at various ratios of polymer to salt: Δ, 8:1; O, 5:1; □, 3:1. a) Crystalline material. Measurements made starting at room temperature and heating to 100°C. Dashed line indicates conductivity in the amorphous phase shown in more detail in b. b) Amorphous material. After quenching the sample from 100°C to room temperature, conductivities were measured starting at room temperature and heating to 100°C.

Fig. 8. Plot of the imaginary part vs. the real part of the admittance (Y) for $PEO \cdot NH_4SO_3CF_3$ 5:1. a) With Pt electrodes at 45°C. b) With ammonium tungsten bronze electrodes at 43°C. The equivalent circuits corresponding to cases a) and b) are shown with circuit elements: bulk resistance, R; geometric capacitance, C geom; double layer capacitance C dl.

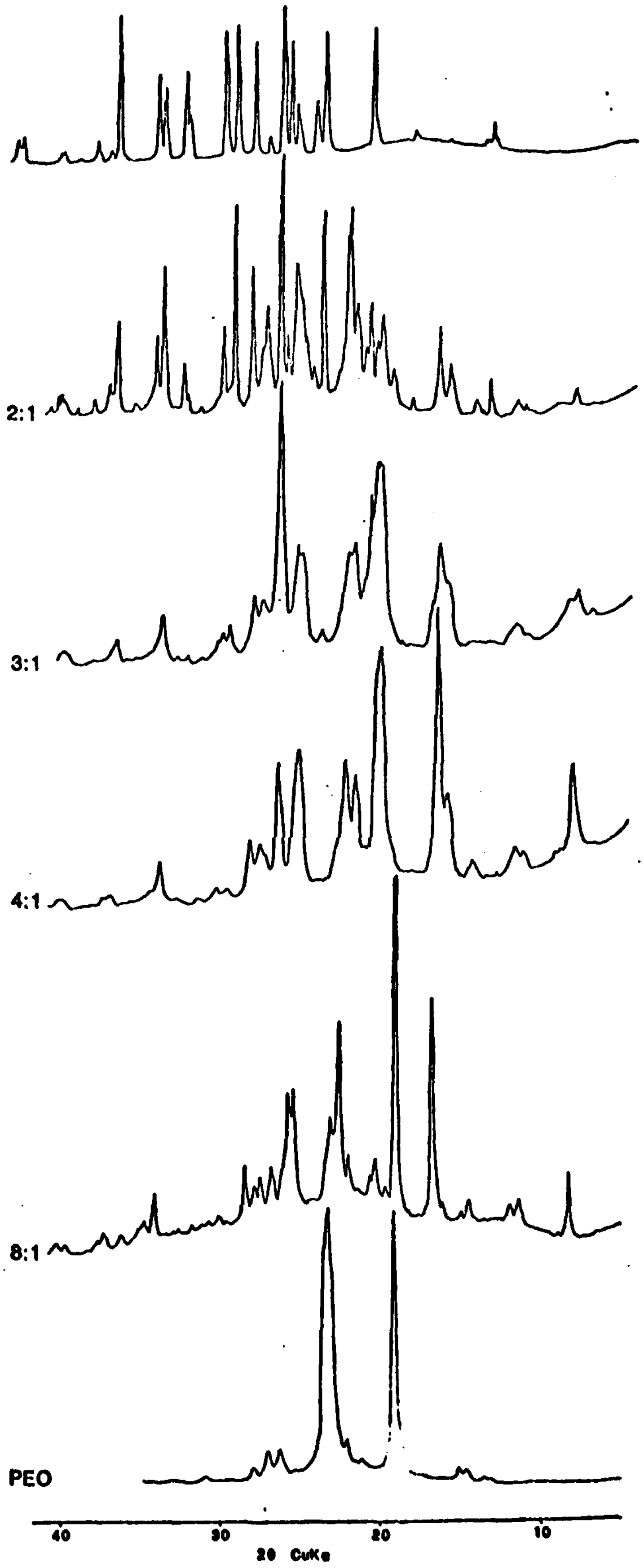
2:1
3:1
4:1
8:1
PEO
40
30
20
10
2θ CuKα

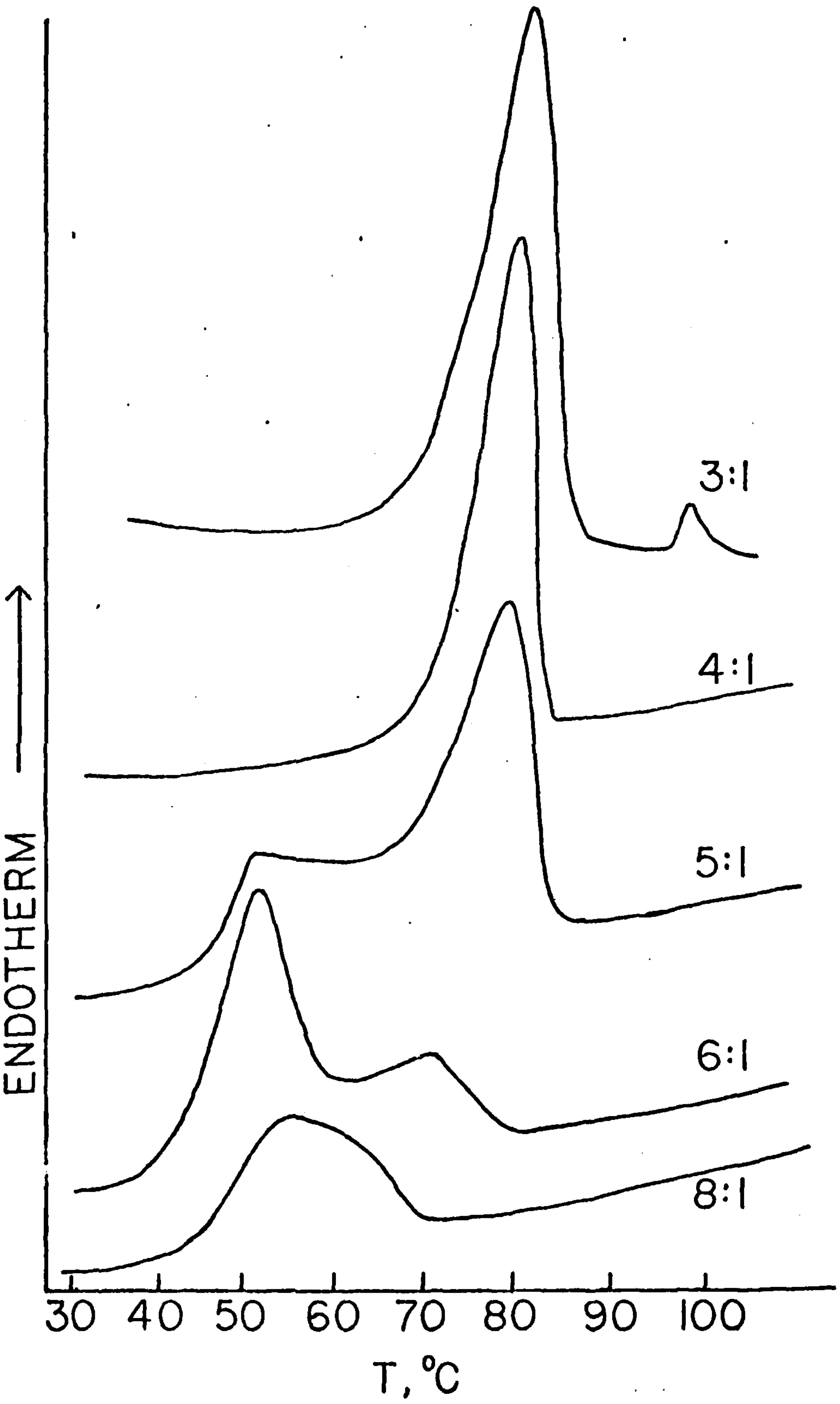
3:1
4:1
5:1
6:1
8:1
ENDOTHERM
30
40
50
60
70
80
90
100
T, °C

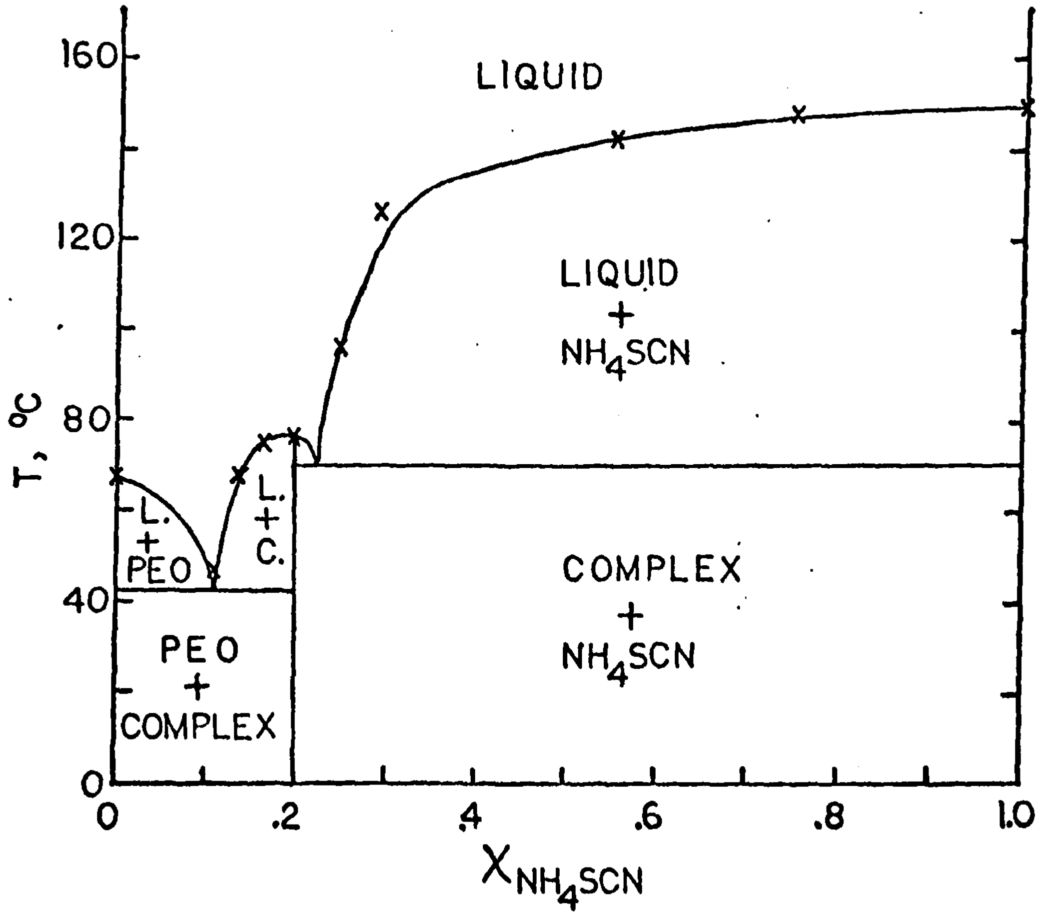
LIQUID
LIQUID + NH$_4$SCN
L. + PEO
L. + C.
PEO + COMPLEX
COMPLEX + NH$_4$SCN
160
120
80
40
0
T, °C
0
.2
.4
.6
.8
1.0
X$_{NH_4SCN}$

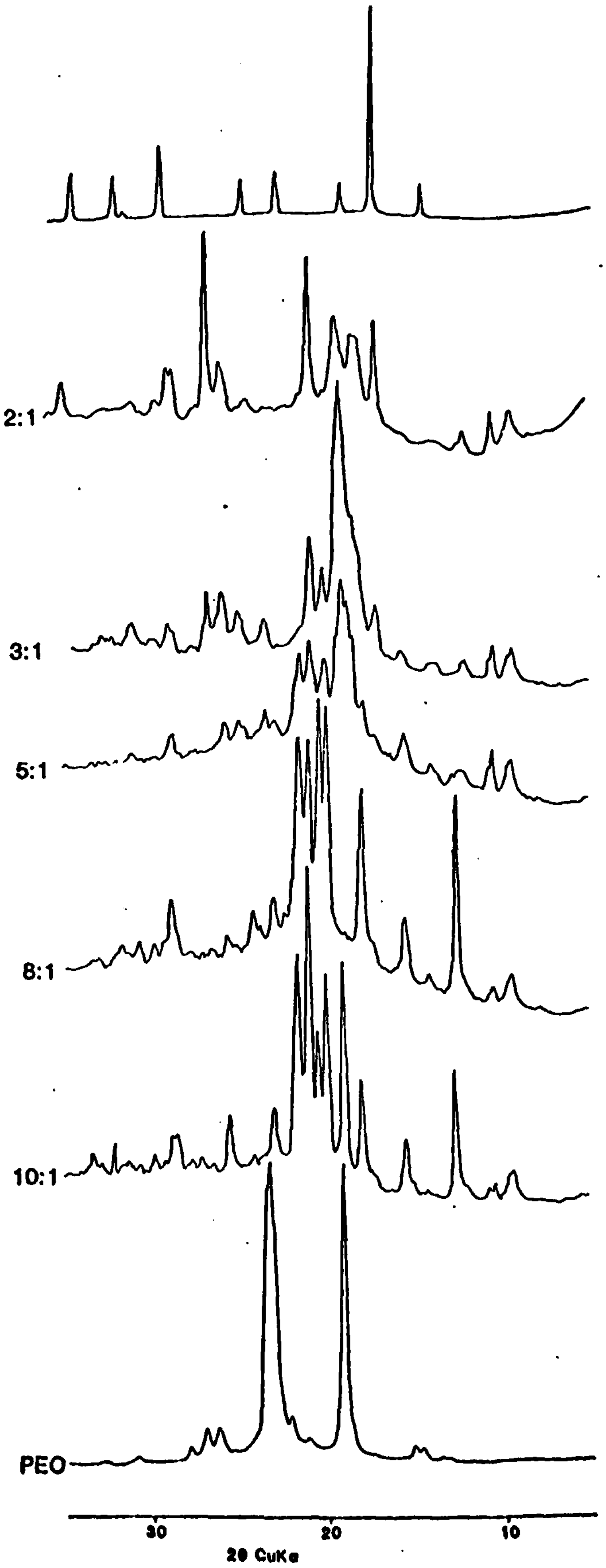
2:1
3:1
5:1
8:1
10:1
PEO
30
20
10
2θ CuKα

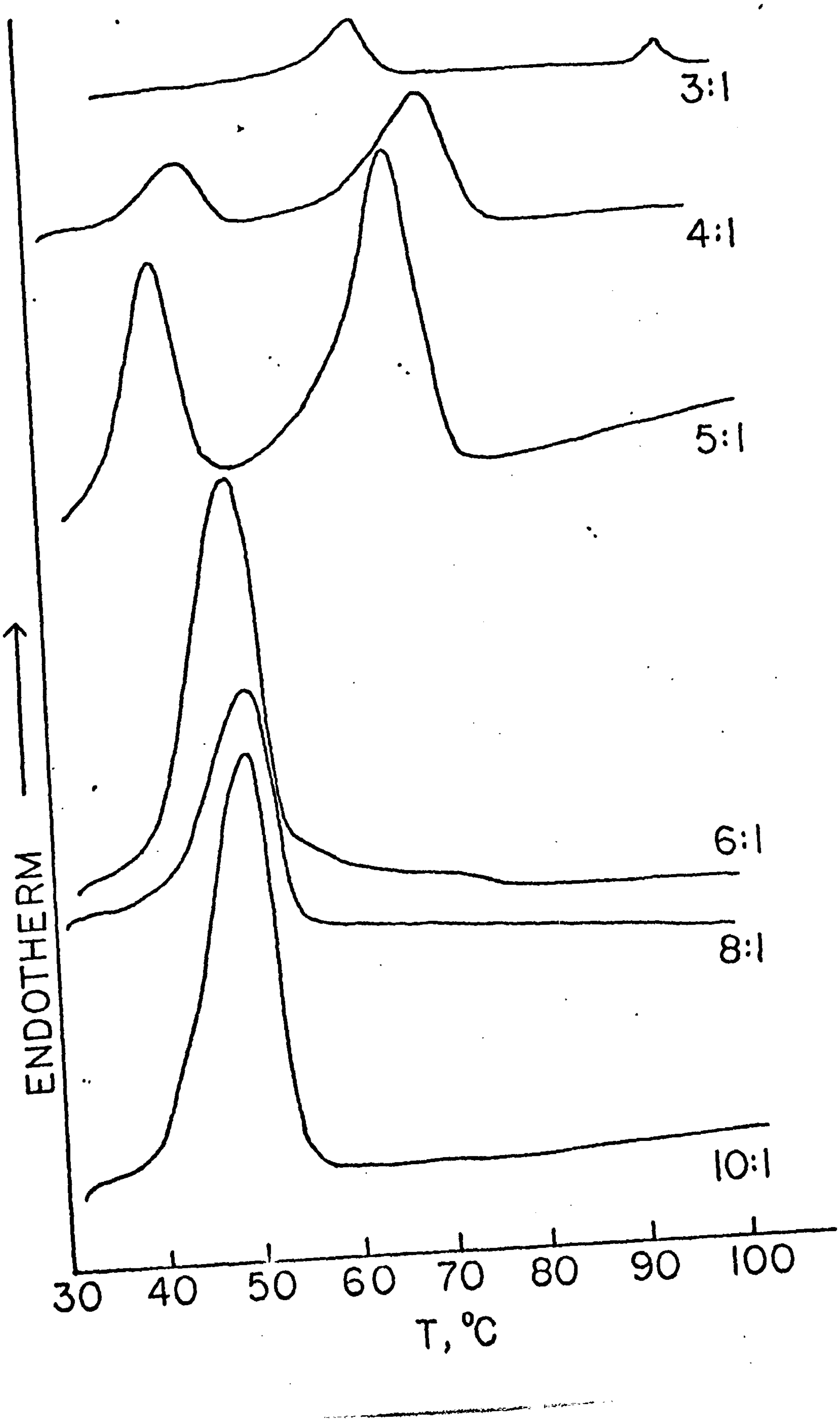
3:1
4:1
5:1
6:1
8:1
10:1
ENDOTHERM
30
40
50
60
70
80
90
100
T, °C

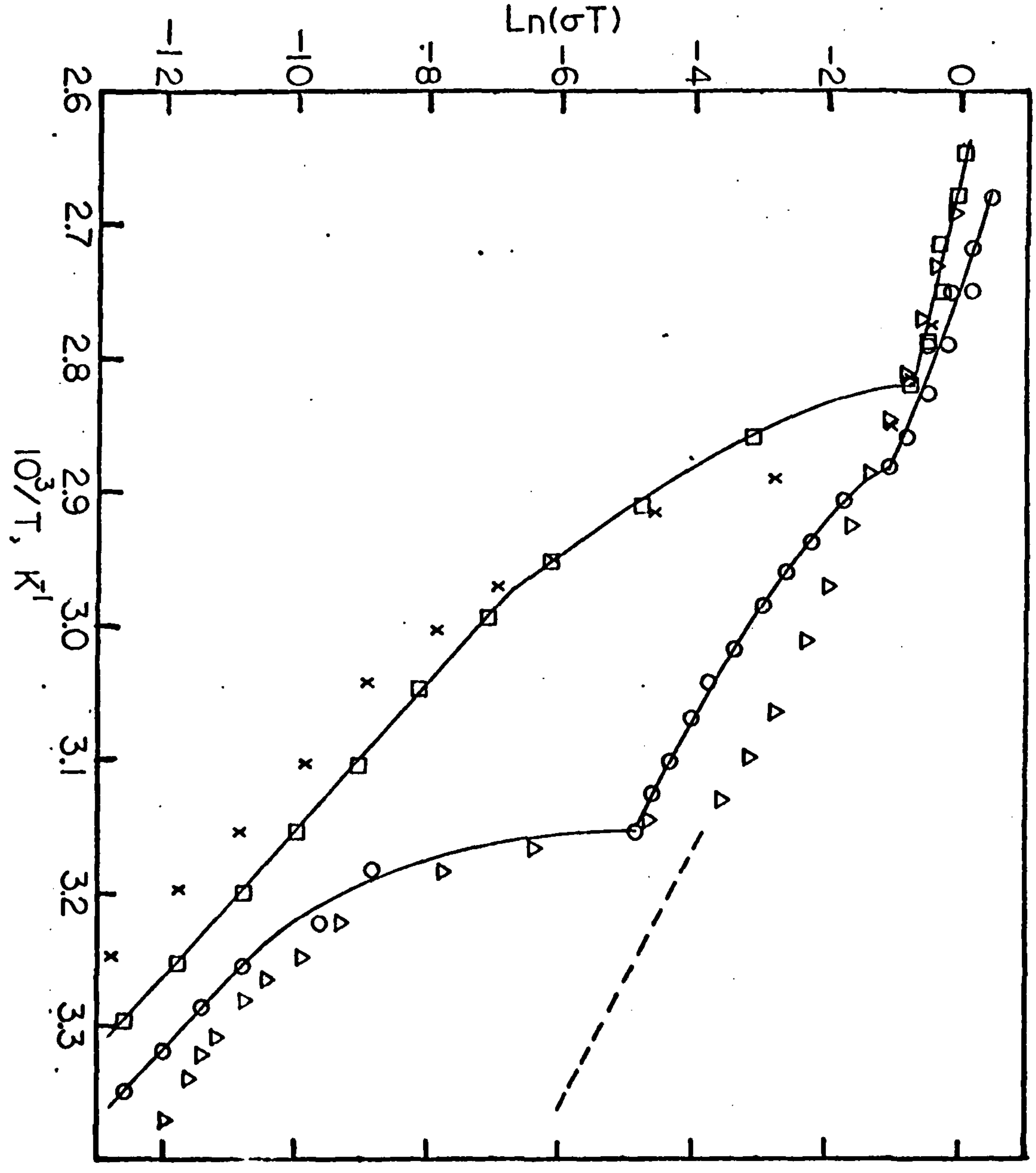
Ln(σT)
0
-2
-4
-6
-8
-10
-12
2.6
2.7
2.8
2.9
3.0
3.1
3.2
3.3
10³/T, K⁻¹

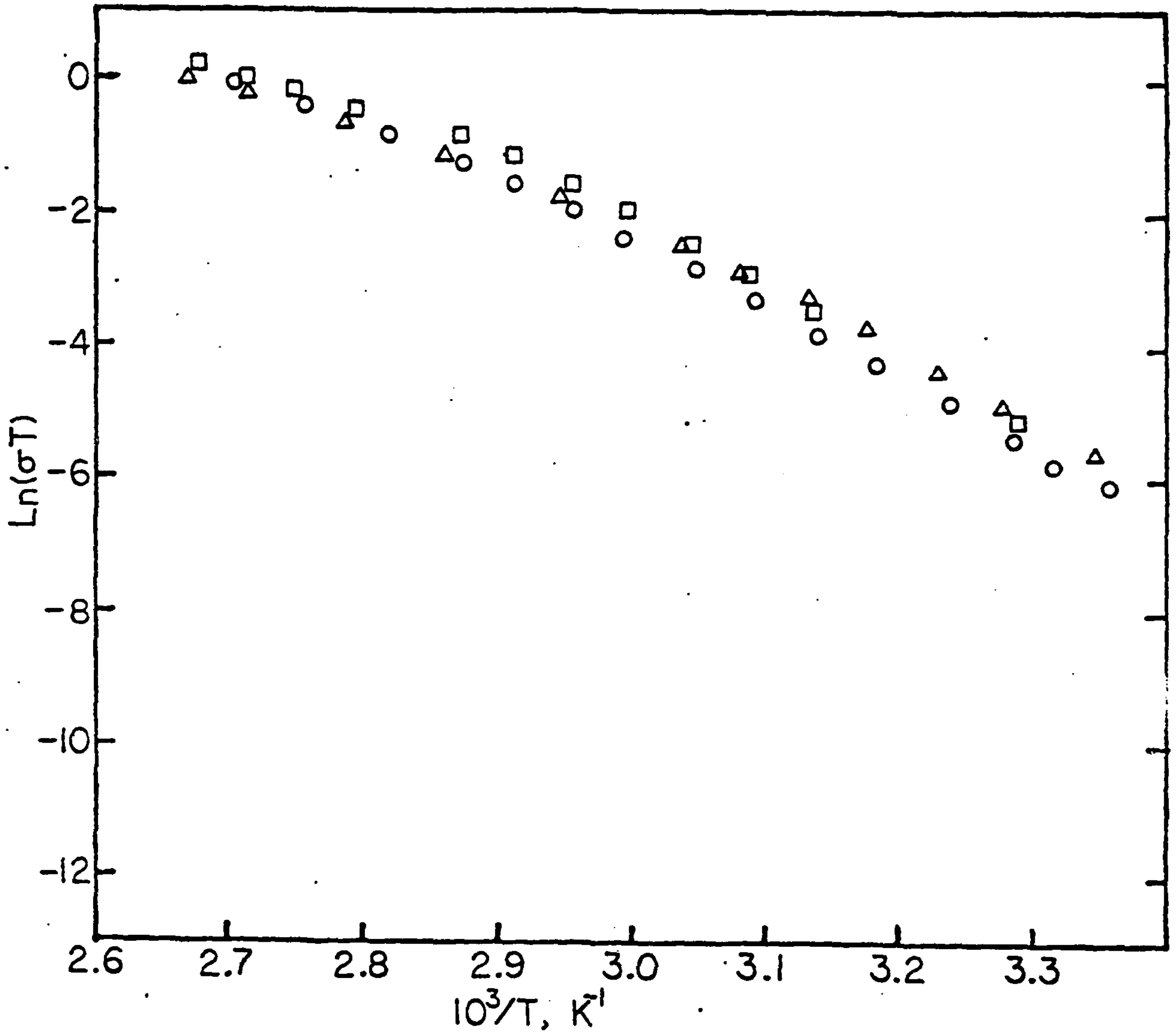

Ln(σT)
0
-2
-4
-6
-8
-10
-12
2.6
2.7
2.8
2.9
3.0
3.1
3.2
3.3
10³/T, K⁻¹

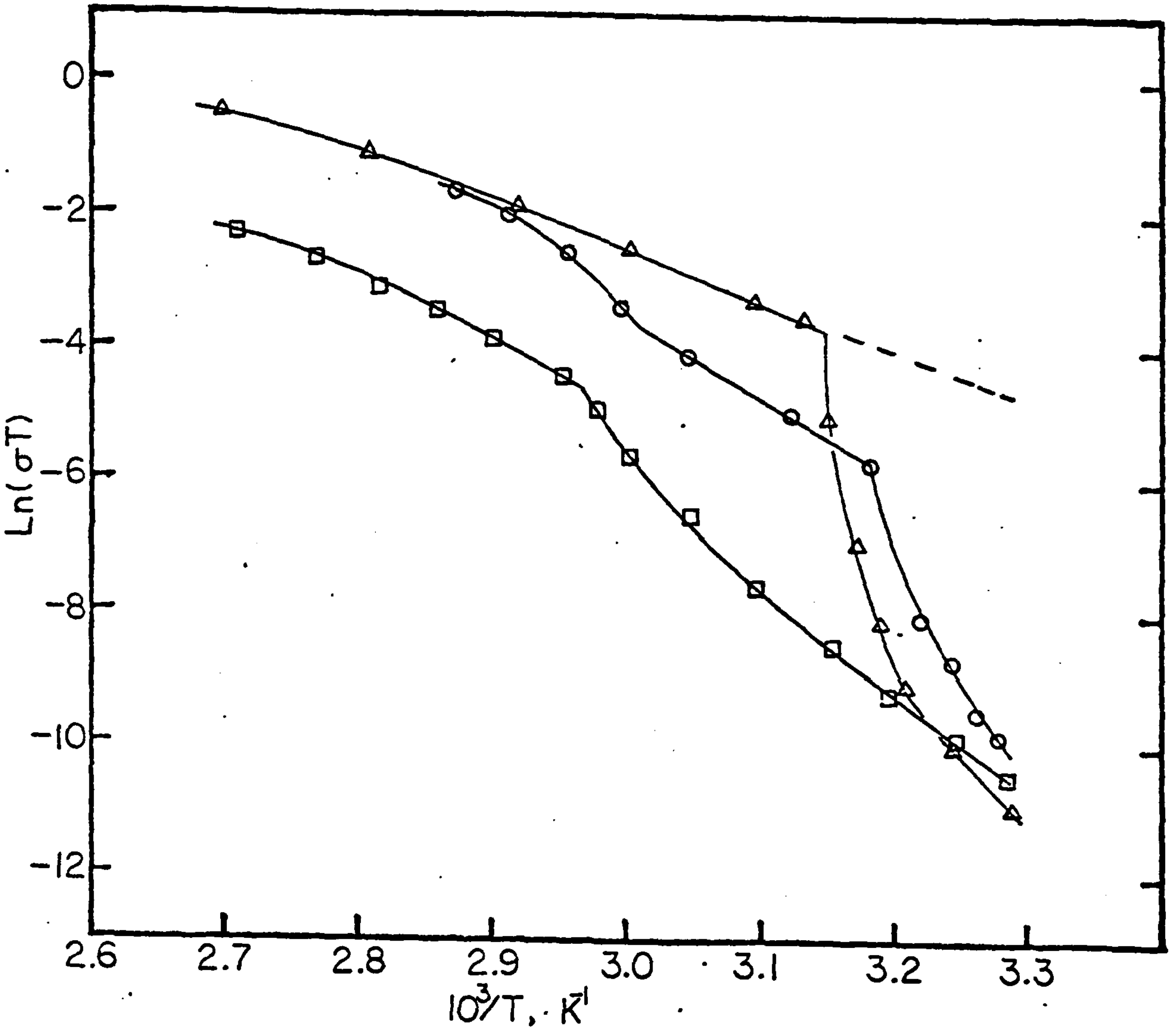
Ln(σT)
0
-2
-4
-6
-8
-10
-12
2.6
2.7
2.8
2.9
3.0
3.1
3.2
3.3
10³/T, K⁻¹

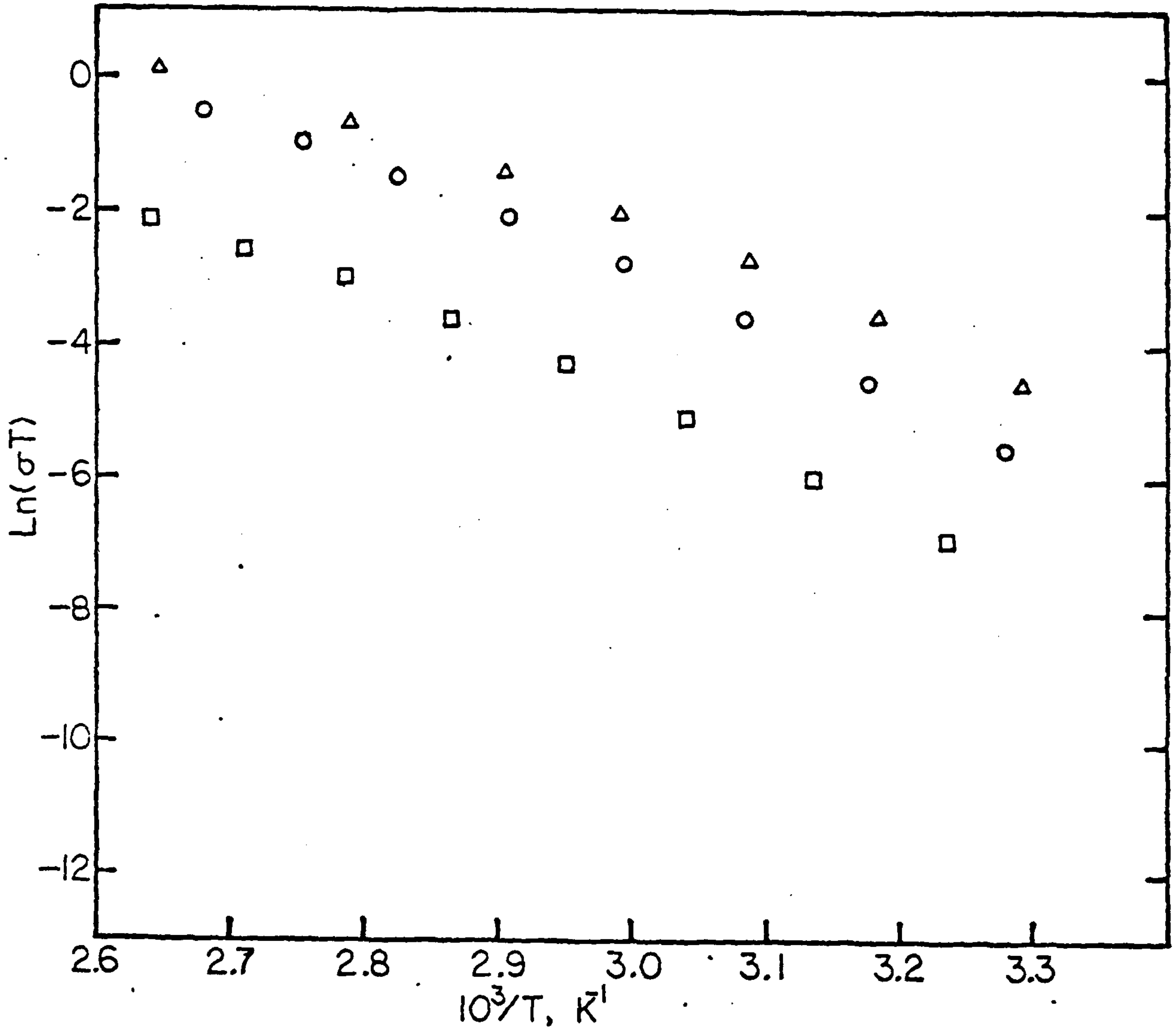
Ln(σT)
0
−2
−4
−6
−8
−10
−12
2.6
2.7
2.8
2.9
3.0
3.1
3.2
3.3
10³/T, K⁻¹

Pt Electrodes , 43°C

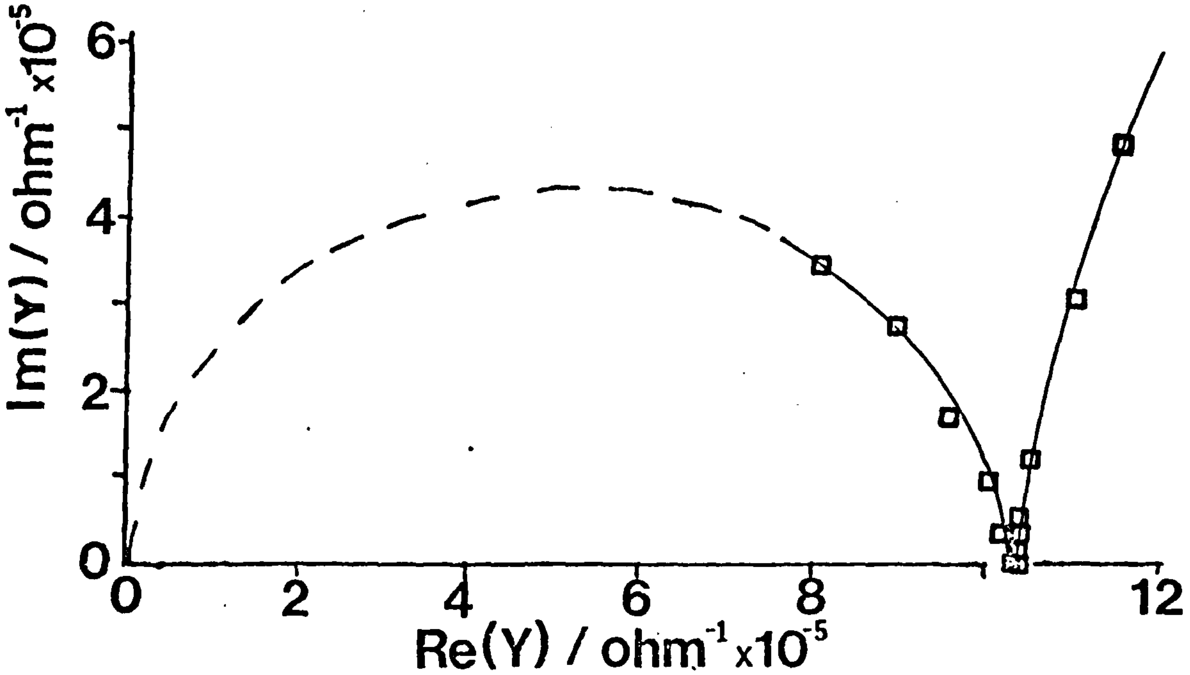

Equivalent circuit

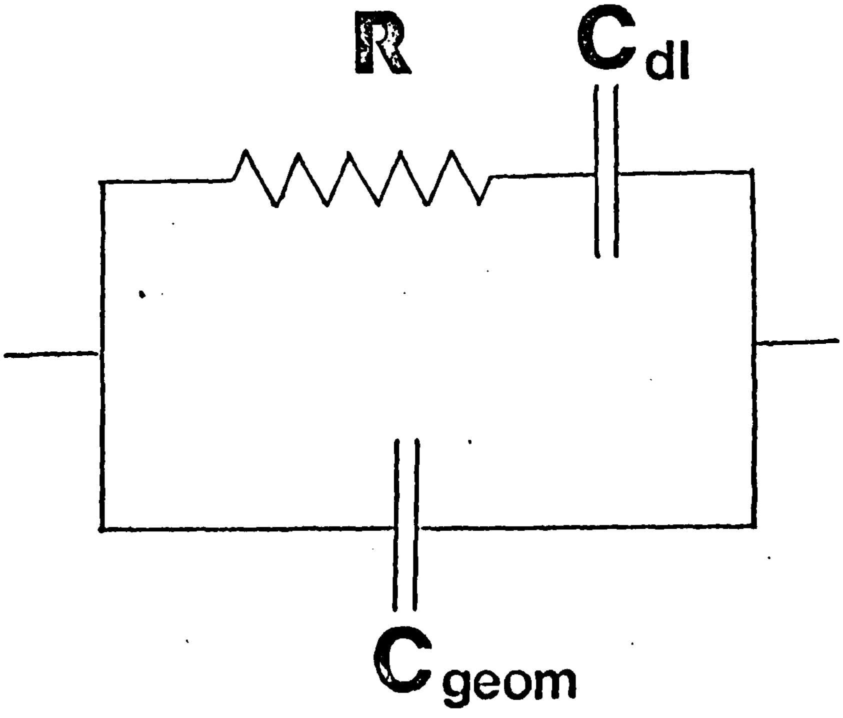

(a)

$(NH_4)_{0.25}WO_3$ Electrodes , 45°C

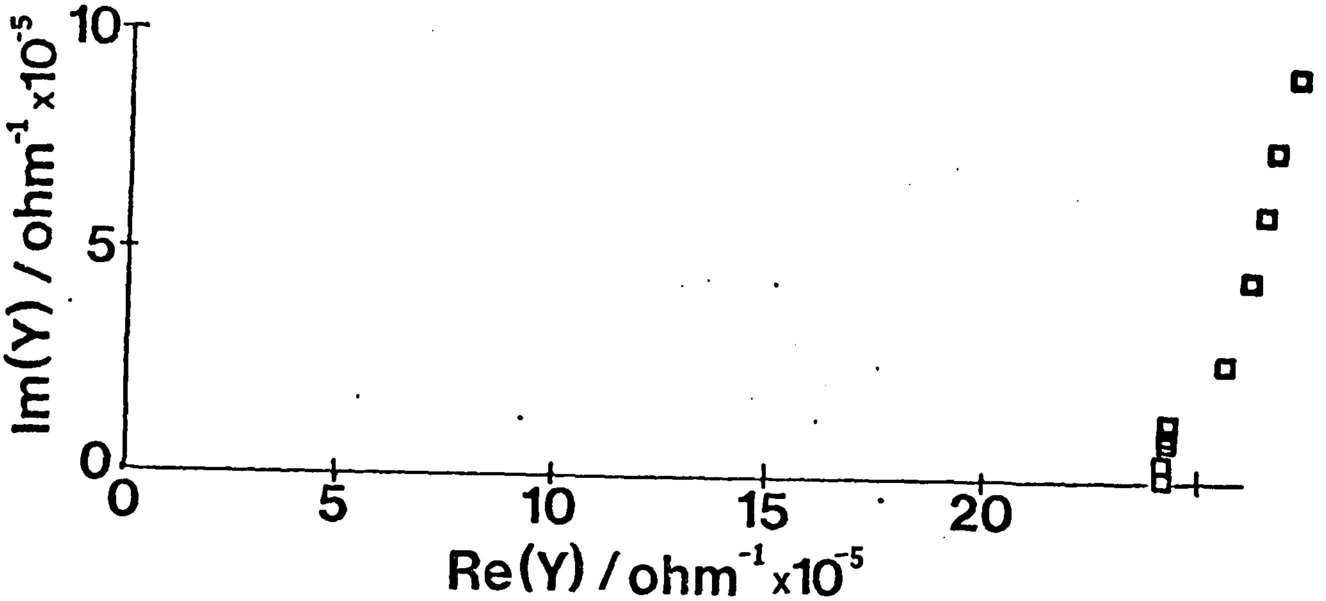

Equivalent circuit

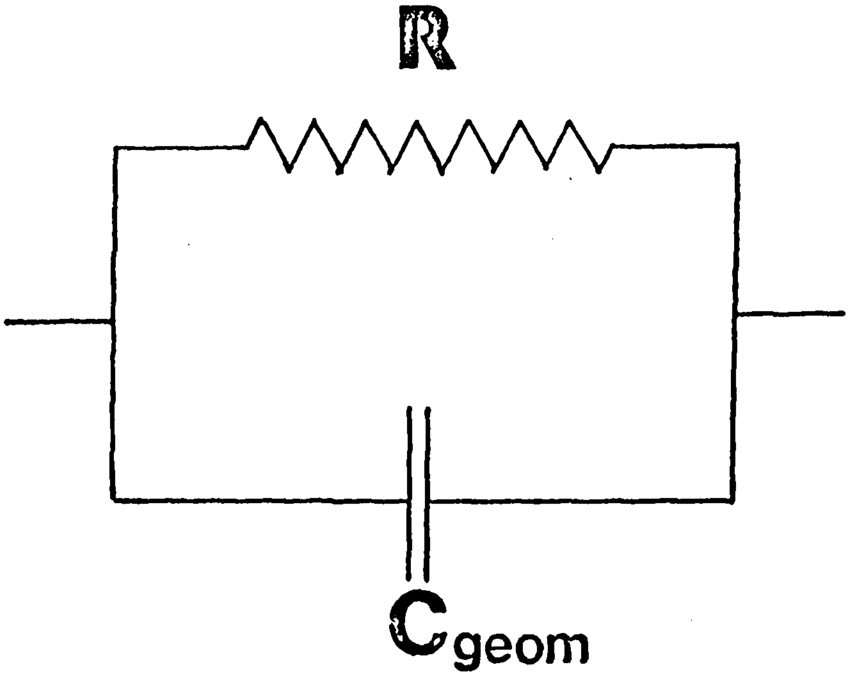

(b)